

**P15R.1 THE DETECTABILITY OF TORNADIC SIGNATURES WITH DOPPLER RADAR:
A RADAR EMULATOR STUDY**

Ryan M. May*, Michael I. Biggerstaff and Ming Xue
University of Oklahoma, Norman, Oklahoma

1. INTRODUCTION

The design of a weather radar system, as well as its scanning strategies, involves various tradeoffs based upon the goal of observing certain features of interest. The tradeoffs made in this design are based on certain assumptions about the performance of the radar system and on characteristics of the feature of interest. Often, the development of algorithms and optimal scanning strategies requires large datasets to test the range of operating parameters and find those that yield the best results. By simulating the operation of a radar, using a software radar emulator, one can artificially generate large data sets that span the range of radar operating characteristics. These generated datasets are attained much more quickly and with less effort than would otherwise be expended in collecting actual data spanning such characteristics.

Many approaches have been taken previously in simulating radar data, varying in sophistication from reflectivity calculation to full simulation of radar returns from each pulse. Krajewski et al. (1993) calculated values of reflectivity factor and differential reflectivity from rainfall rates from a numerical model, using an assumed drop size distribution. Similarly, Chandrasekar and Bringi (1987) looked at the variation of simulated reflectivity values as a function of raindrop size distribution parameters. Neither of these studies was concerned with the Doppler velocity information. Wood and Brown (1997) evaluated the effects of WSR-88D (Weather Surveillance Radar-1988 Doppler) scanning strategies on the sampling of mesocyclones and tornadoes. The effects of the scanning strategy were accounted for by using an effective beamwidth for the radar that was used to scan an analytic vortex. Capsoni and D'Amico (1998) simulated the pulse to pulse time series of radar data by combining the

simulated returns from individual hydrometeors within a radar volume. Due to the computational requirements of this approach, the radar data were generated for only a single range gate, and thus the aspects of scanning the radar were not simulated.

This work describes a radar emulator designed to simulate the returns from a scanning Doppler radar on a pulse to pulse basis. Starting with output from a high resolution numerical simulation of a supercell thunderstorm (Xue 2004), the emulator generates radar reflectivity, Doppler velocity, and Doppler spectrum width, based on the configured radar and scanning strategy. This emulator is capable of simulating many of the impacts of radar and scanning strategy design on the resolution and quality of collected data. The application of this emulator to studying the detectability of tornadoes by broad-beam, low power radars is shown as an example of the utility of this tool.

2. EMULATOR DESIGN

The operation of the emulator is controlled by two separate sets of parameters which describe the radar and the scanning strategy. The parameters that describe the radar are: location of the radar relative to the numerical simulation grid, antenna beamwidth, antenna gain, wavelength, transmit power, range to the first radar gate, and the minimum detectable signal. The parameters that describe the scanning strategy are: pulse repetition time (PRT), pulse length, antenna rotation rate, number of pulses to average to produce a radial, the spacing between radar gates, and the necessary antenna pointing angles.

Input into the emulator are the numerical grids from a high resolution numerical simulation. There is no required resolution for these grids, but the spatial resolution of the model fields should be

* *Corresponding author address:* Ryan M. May
Univ. of Oklahoma, School of Meteorology
100 East Boyd St. Suite 1310 Norman, OK 73019
e-mail: rmay@rossby.ou.edu.

better than the resolution of the radar being emulated. The meteorological variables used by the radar emulator are: three dimensional wind components, density of hydrometeors (rain and cloud water), and temperature. In this work, the input used is a simulation of a tornadic thunderstorm produced by the Advanced Regional Prediction System (ARPS) (Xue 2004, Xue et al. 2000). This particular simulation used warm-phase microphysics and was run on a 50m horizontal grid spacing and a stretched vertical grid spacing, with 20m the spacing at the surface.

The emulator calculates the power returned to the radar by a simulated pulse, which is propagated through the numerical grid, using the standard radar equation (Doviak and Zrníc 1993):

$$\bar{P}(r_0) = \frac{P_t g^2 \lambda^4}{(4\pi)^3} \sum_{all\ i} \frac{f_i^4 W_i^2 \eta_i V_i}{l_i^2 r_i^2} \quad (1)$$

where P_t is the transmit power, g is the antenna gain, λ is the wavelength, f is the normalized antenna gain, W is the range weighting, η is the reflectivity, l is the attenuation coefficient, and r is the range. Quantities with the i subscript represent individual contributions to the simulated pulse. The reflectivity is calculated from the model's rain water and cloud water concentrations, using the Rayleigh approximation. The rain water is assumed to have a Marshall-Palmer (1948) distribution, while cloud water is assumed to be monodisperse. Attenuation is also calculated using the extinction cross section from Rayleigh scattering, including the temperature and wavelength dependencies of the index of refraction of water.

From this returned power, and the model's three dimensional velocity field, the emulator calculates equivalent reflectivity factor (Z_e), Doppler velocity, and Doppler spectrum width. Z_e is calculated as (Doviak and Zrníc 1993):

$$Z_e = \frac{2^{10} \ln(2) \lambda^2 r^2 \bar{P}_r}{\pi^3 P_t g^2 \theta_1^2 c \tau |K_w|^2} \quad (2)$$

where P_r is the returned power, θ_1 is the 3dB beamwidth, c is the speed of light, τ is the pulse length, and $|K_w|^2$ is approximately 0.93. Doppler

velocity is calculated as the power-weighted average of the radial velocities within the pulses, while Doppler spectrum width is calculated as the standard deviation of radial velocities within the pulse.

The combination of the configuration options above with the described physics allows for the simulation of over- and under-sampling in azimuth, gate spacing, velocity aliasing, range aliasing, antenna beamwidth with sidelobes, and frequency-dependent attenuation. As an example of the basic output from the emulator, Figure 1 shows a Plan Position Indicator (PPI) of equivalent reflectivity factor (Z_e) from an emulated WSR-88D radar.

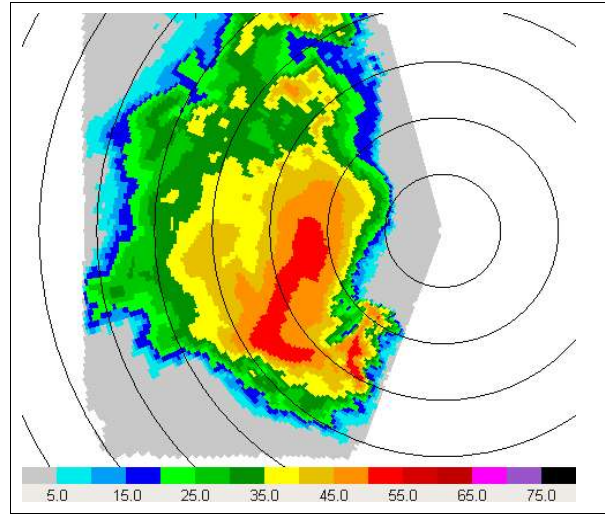


Figure 1: PPI of Z_e (in dBZ) for an emulated WSR-88D radar. Range rings are plotted every 5km from the radar.

2.1 Wavelength and Attenuation

To show the effects of transmit wavelength on an emulated radar, the emulator was run with the same WSR-88D parameters as before, but with a 3cm transmit wavelength. A PPI of Z_e from this run are shown in Figure 2. It is also possible to look at the difference in Z_e between the two runs, which is shown in Figure 3. This figure shows clearly a region where the values of Z_e at 3cm are much lower than those at 10cm, with differences on the order of 10dB in this region.

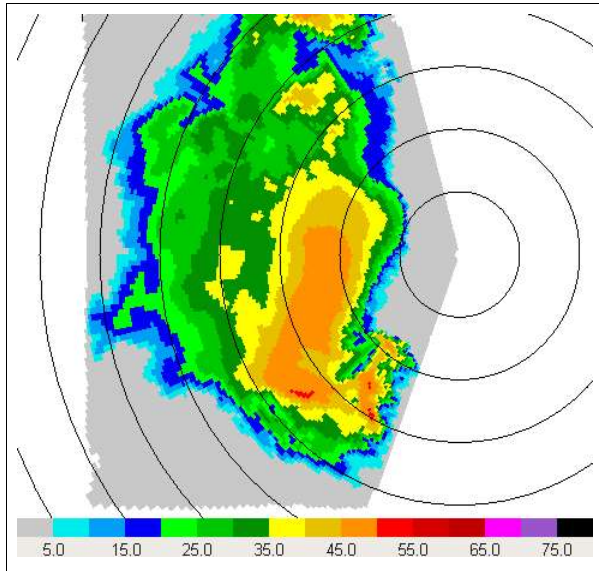


Figure 2: PPI of Z_e (in dBZ) for an emulated WSR-88D operating at 3cm wavelength. Range rings are plotted every 5km.

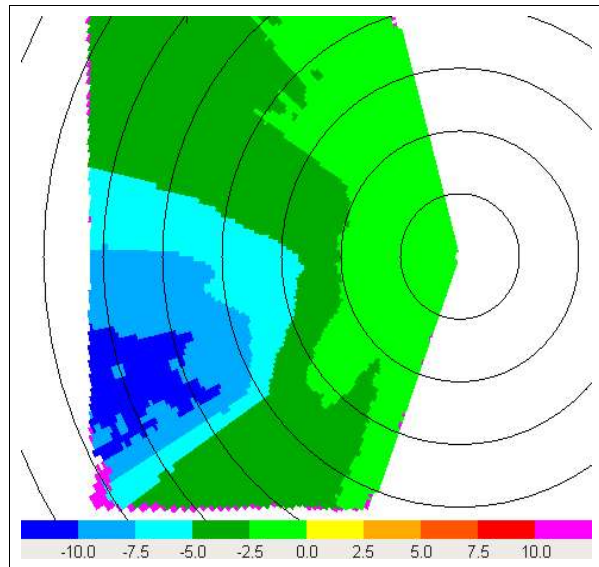


Figure 3: Z_e for WSR-88D minus Z_e for 3cm WSR-88D. Range rings are plotted every 5km.

2.2 2nd Trip Echoes

The previous WSR-88D run can be modified to place the radar 110km from the edge of the storm and set the unambiguous range to 117km. With these settings, part of the storm lies beyond the unambiguous range, and 2nd trip returns are recorded. Such returns are evident in Figure 4, a PPI of Z_e . These returns have much weaker reflectivity values and are much smaller in extent than the actual storm. This is due to noise thresholding based on power, and because reflectivity is miscalculated from power as a result of being assigned the incorrect range.

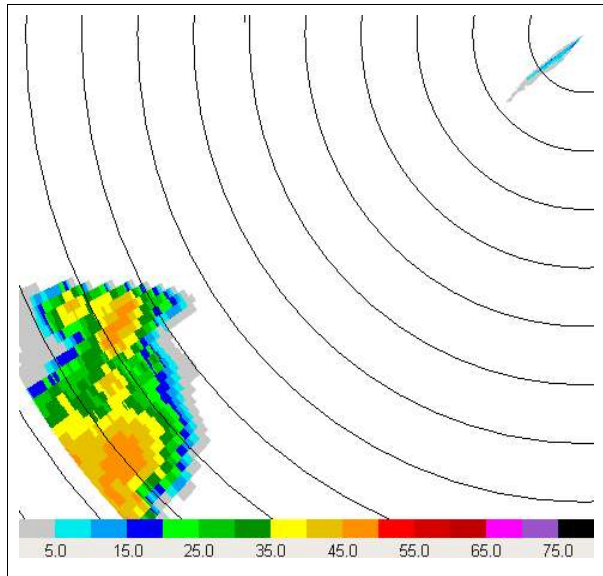


Figure 4: Z_e for emulated WSR-88D showing 2nd trip echoes. Range rings are plotted every 10km.

3. APPLICATION TO DETECTABILITY OF TORNADOES

The radar emulator described above was used to examine the impacts of radar and scanning strategy characteristics on the detection of tornadic circulations. The input numerical simulation for the emulator is the same as described above. This simulated storm produced a strong tornado 200m across, with a velocity difference of 160ms^{-1} across the tornado, which corresponds to F3 on the Fujita scale.

The study here focuses on the ability to detect tornadic circulations using low-power, X-band

radars with 2° beamwidths. Radars of this type are planned to be deployed as part of a prototype network in central Oklahoma, through the Collaborative Adaptive Sensing of the Atmosphere (CASA) project, a National Science Foundation Engineering Research Center (Brotzge et al. 2005).

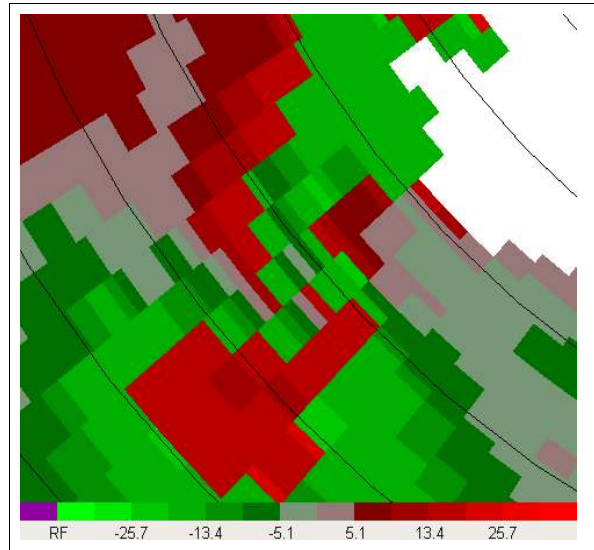
To objectively quantify the impacts of radar and scanning strategy characteristics, several metrics have been chosen to measure radar's detection of the tornado: width (L), change in velocity across circulation (ΔV), and the vorticity parameter. The vorticity parameter is defined as $2\Delta V/L$, and is equal to the vorticity for an axisymmetric vortex. The baseline values for these parameters, taken from the simulation itself, are a value of 200m for L, 160ms^{-1} for ΔV , and 1.6s^{-1} for $2\Delta V/L$.

Unless otherwise specified, the data here was generated using the parameters specified in Table 1. It should be noted that attenuation is not actually employed in these runs. However, due to the viewing angle of the radar to the tornado, the effects of attenuation would be negligible. A PPI of Doppler velocity for these parameters is shown in Figure 5, magnified in to show detail of the tornadic circulation.

Using the radar characteristics specified in Table 1, several runs were performed, varying range to the storm, elevation angle, azimuthal sampling interval, and Nyquist velocity. The results from these runs are summarized in Table 2. It was found that a sharp degradation in the metrics occurred as the range to the tornado increases. By 20km range, the size of the circulation measured by the radar is 538m, and the

Wavelength	3cm
3dB Beamwidth	2°
Gate Spacing	100m
Nyquist Velocity	18.75ms^{-1}
Unambiguous Range	60km
Radial Spacing	2°
Range to Storm	10km
Elevation Angle	0.5°

Table 1: Parameters for emulated CASA radars.



Figures 5: PPI of Doppler velocity for an emulated CASA radar. Range rings are plotted every 1km.

vorticity parameter has decreased to 0.14s^{-1} . This degradation is primarily a result of the mainlobe of the radar beam being 698m across at this range.

A second feature noticeable in Table 2 is how fast the metrics degrade from their baseline values. Even at 3km, the vorticity parameter has decreased to a value of 0.6s^{-1} . Three kilometers is close for a fixed-site radar. It is interesting to note that even at this range, the vorticity parameter has already degraded to one third of its baseline value.

Overall, it is clear that range is a significant issue in the ability of broad-beam radars to detect tornadic circulations. However, the degradation of these metrics as range increases can be offset somewhat by azimuthal oversampling, or sampling with a radial spacing greater than the beamwidth. This sampling showed some modest gains at 10km, and would probably show even better improvement over matched sampling at 20km.

It is also important to note that some preliminary runs were also conducted using a model simulation time that contained a strong mesocyclonic circulation, but no tornado. The emulated CASA radar could easily distinguish between this case and the case with the tornadic circulation, which provides some indication that the radars might be useful in improving false alarm rates for tornado detection.

<i>Run</i>	<i>Max V In</i>	<i>Max V Out</i>	<i>L</i>	ΔV	$2\Delta V/L$
	(ms ⁻¹)	(ms ⁻¹)	(m)	(ms ⁻¹)	(s ⁻¹)
3km Range, 0.0° Elevation	31.6	31.3	229	62.9	0.55
3km Range	31.6	30.6	229	62.2	0.54
3km Range, 1.0° Elevation	28.3	32.7	202	61	0.6
10km Range, 0.0° Elevation	29.7	34.3	368	64	0.35
10km Range	23.3	34.4	368	57.7	0.31
10km Range, 1.0° Elevation	21.1	37.2	368	58.3	0.32
10km Range, 25ms ⁻¹ Nyquist	19.6	22.9	363	42.5	0.23
10km Range, 1° Radial Spacing	27.1	34.5	352	61.6	0.35
10km Range, 3° Radial Spacing	19.1	28.8	538	47.9	0.18
20km Range	13.5	35	710	48.5	0.14
30km Range	14	33.4	1080	47.4	0.09

Table 2: Summary of tornadic circulation metrics for set of emulated CASA radars.

4. CONCLUSIONS

A software radar emulator has been created that is useful for researching the impact of radar network and scanning strategy characteristics. The emulator's capabilities include simulating azimuthal over- and under-sampling, attenuation, antenna beamwidth with sidelobes, gate spacing, and 2nd trip echoes. As an example application, the emulator was used to quantify the ability of low-power, broad-beam X-band radars to detect tornadic circulations. Range will be a significant issue in the detectability, due to their large beamwidth, but they show some utility in differentiating between mesocyclonic and tornadic circulations.

5. ACKNOWLEDGMENTS

Support for this project was provided by graduate research fellowships sponsored by the Office of Naval Research through the American Meteorological Society and by the Army Research Office through the National Defense Science and Engineering Graduate Fellowship program. Partial support was also provided by the National Science Foundation through the Engineering Research Center Grant #EEC-0313747.

6. REFERENCES

- Brotzge, J. A., K. Brewster, B. Johnson, B. Philips, M. Preston, D. Westbrook, and M. Zink, 2005: CASA's first testbed: Integrated project #1 (IP1). *Preprints, 32nd Conf. on Radar Meteor.* Albuquerque, New Mexico.
- Capsoni, C., and M. D'Amico, 1998: A physically based radar simulator. *J. Atmos. Oceanic Technol.*, **15**, 593-598.
- Chandrasekar, V., and V. N. Bringi, 1987: Simulation of radar reflectivity and surface measurements of rainfall. *J. Atmos. Oceanic Technol.*, **4**, 464-478.
- Doviak, R. J., and D. S. Zrnic, 1993: *Doppler Radar and Weather Observations*. Academic Press, San Diego, 562pp.
- Krajewski, W. F., R. Raghavan, and V. Chandrasekar, 1993: Physically based simulation of radar rainfall data using a space-time rainfall model. *J. Appl. Meteor.* **32**, 268-283.
- Marshall, J. S., and W. M. Palmer, 1948: The distribution of raindrops with size. *J. Meteor.*, **5**, 165-165.
- Wood, V. T., and R. A. Brown, 1997: Effects of radar sampling on single-Doppler velocity signatures of mesocyclones and tornadoes. *Wea. Forecasting*, **12**, 928-938.
- [Xue, M., K. K. Droegemeier, and V. Wong, 2000:](#)

The Advanced Regional Prediction System (ARPS) - A multiscale nonhydrostatic atmospheric simulation and prediction tool. Part I: Model dynamics and verification. *Meteor. Atmos. Physics.* **75**, 161-193.

Xue, Ming, 2004: Tornadogenesis within a simulated supercell thunderstorm. Preprints, *22nd Conf. on Severe Local Storms, Hyannis, Massachusetts.*